Carbon isotope ratio of Cenozoic CO_2: A comparative evaluation of available geochemical proxies

Brett J. Tipple,[1,2] Stephen R. Meyers,[3] and Mark Pagani[1]

Received 21 August 2009; revised 16 February 2010; accepted 1 March 2010; published 17 July 2010.

[1] The carbon isotope ratio ($\delta^{13}C$) of plant material is commonly used to reconstruct the relative distribution of C_3 and C_4 plants in ancient ecosystems. However, such estimates depend on the $\delta^{13}C$ of atmospheric CO_2 ($\delta^{13}C_{CO2}$) at the time, which likely varied throughout Earth history. For this study, we use benthic and planktonic $\delta^{13}C$ and $\delta^{18}O$ records to reconstruct a long-term record of Cenozoic $\delta^{13}C_{CO2}$. Confidence intervals for $\delta^{13}C_{CO2}$ values are assigned after careful consideration of equilibrium and non-equilibrium isotope effects and processes, as well as resolution of the data. We find that benthic foraminifera better constrain $\delta^{13}C_{CO2}$ compared to planktonic foraminiferal records, which are influenced by photosymbiotes, depth of production, seasonal variability, and preservation. Furthermore, sensitivity analyses designed to quantify the effects of temperature uncertainty and diagenesis on benthic foraminifera $\delta^{13}C$ and $\delta^{18}O$ values indicate that these factors act to offset one another. Our reconstruction suggests that Cenozoic $\delta^{13}C_{CO2}$ averaged -6.1 ± 0.6‰ (1σ), while only 11.2 million of the last 65.5 million years correspond to the pre-Industrial value of −6.5‰ (with 90% confidence). Here $\delta^{13}C_{CO2}$ also displays significant variations throughout the record, at times departing from the pre-Industrial value by more than 2‰. Thus, the observed variability in $\delta^{13}C_{CO2}$ should be considered in isotopic reconstructions of ancient terrestrial-plant ecosystems, especially during the Late and Middle Miocene, times of presumed C_4 grassland expansion.

Citation: Tipple, B. J., S. R. Meyers, and M. Pagani (2010), Carbon isotope ratio of Cenozoic CO_2: A comparative evaluation of available geochemical proxies, *Paleoceanography*, *25*, PA3202, doi:10.1029/2009PA001851.

1. Introduction

[2] The $\delta^{13}C$ value of atmospheric CO_2 ($\delta^{13}C_{CO2}$), along with isotopic fractionations associated with carbon fixation and a plant's specific water use efficiency, determine terrestrial plant carbon isotopic compositions [*Farquhar et al.*, 1989]. Precise measurements of $\delta^{13}C_{CO2}$ and plant $\delta^{13}C$ values are readily available for modern canopy and leaf-scale research [*Lai et al.*, 2006; *Pypker et al.*, 2008], and allow the relative abundance of C_3 and C_4 plants in various environments to be accurately determined by stable carbon isotope analysis of sedimentary organic carbon [*Follett et al.*, 2009; *Wang et al.*, 2010]. Ice core measurements of $\delta^{13}C_{CO2}$ are only available for the last 50 kyr [*Elsig et al.*, 2009; *Friedli et al.*, 1986; *Leuenberger et al.*, 1992; *Smith et al.*, 1999]. Consequently, the value of $\delta^{13}C_{CO2}$ must be assumed for earlier periods of Earth history in order to establish C_3 and C_4 distributions using the $^{13}C/^{12}C$ compositions of organic carbon.

[3] Carbon fluxes into and out of ocean-atmosphere reservoirs can vary overtime [*Berner*, 1998, 2006; *Kump and Arthur*, 1999], and alter the $\delta^{13}C$ value of individual carbon reservoirs [*Katz et al.*, 2005; *Zachos et al.*, 2001] and the partial pressure of atmospheric carbon dioxide (pCO_2) [*Pagani et al.*, 2005; *Royer et al.*, 2004]. On human timescales, $\delta^{13}C_{CO2}$ has changed by ~−1.5‰ concurrent with the increase in anthropogenic CO_2 since the Industrial Revolution [*Marino et al.*, 1992]. While the $\delta^{13}C_{CO2}$ value has almost assuredly evolved over longer time intervals, terrestrial paleoecologic reconstructions often apply a pre-Industrial $\delta^{13}C_{CO2}$ value of −6.5‰ for geochemical reconstructions of plant distributions, because $\delta^{13}C_{CO2}$ before the late Quaternary is not precisely constrained [*Bibi*, 2007; *Boisserie et al.*, 2005; *Feakins et al.*, 2005; *Feakins et al.*, 2007; *Fox and Koch*, 2003, 2004; *Hopley et al.*, 2007; *Levin et al.*, 2004; *Ségalen et al.*, 2006; *Zazzo et al.*, 2000].

[4] Reconstructions of $\delta^{13}C_{CO2}$ have been developed using $\delta^{13}C$ records of ancient plant matter [*Gröcke*, 2002; *Jahren et al.*, 2001; *Marino et al.*, 1992] and foraminifera [*Passey et al.*, 2009, 2002; *Smith et al.*, 2007]. Long-term (multimillion year) $\delta^{13}C_{CO2}$ reconstructions are often based on the $\delta^{13}C$ of ancient woody material that was subjected to different levels of molecular degradation and thermal maturation [*van Bergen and Poole*, 2002]. As a consequence, interpretations of $\delta^{13}C_{CO2}$ from fossil-wood $\delta^{13}C$ values require a detailed understanding of diagenetic histories – a condition rarely satisfied. Moreover, environmental conditions strongly influence carbon-isotope compositions of

[1]Department of Geology and Geophysics, Yale University, New Haven, Connecticut, USA.
[2]Now at Department of Biology, University of Utah, Salt Lake City, Utah, USA.
[3]Department of Geoscience, University of Wisconsin-Madison, Madison, Wisconsin, USA.

0883-8305/10/2009PA001851

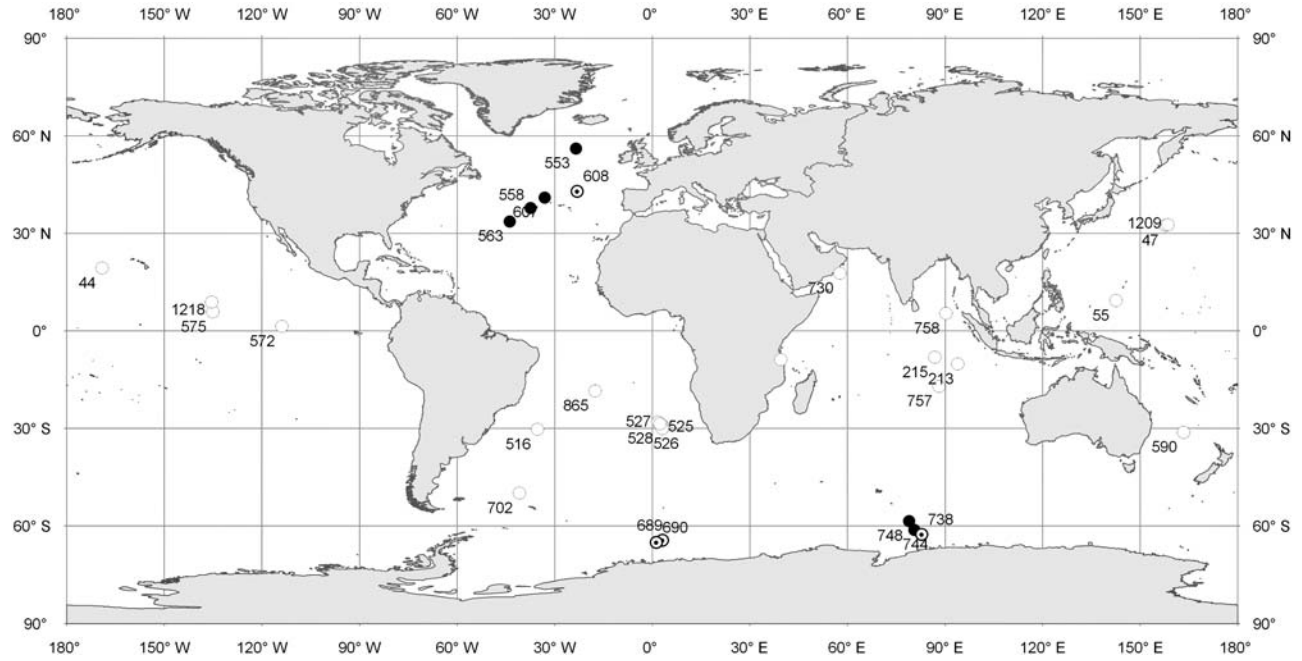

Figure 1. Marine core locations. Cores from which planktonic, benthic, and both planktonic and benthic $\delta^{13}C_{cc}$ records were compiled are shown with open circles, black circles, and circles with dots, respectively.

terrestrial plants, contributing as much as ±5‰ variability [*Deines*, 1980], adding to the uncertainty to $\delta^{13}C_{CO2}$ reconstructions [*Bump et al.*, 2007].

[5] Marine carbonates are abundant and better preserved in comparison to terrestrial organic matter. It is well established that the carbon-isotopic composition of foraminiferal calcite ($\delta^{13}C_{cc}$) is primarily controlled by the $\delta^{13}C$ of dissolved inorganic carbon ($\delta^{13}C_{DIC}$), species-specific biological ('vital') effects, temperature, and pH [*Spero and Lea*, 1993]. Consequently, planktonic and benthic $\delta^{13}C_{cc}$ records are useful in inferring surface productivity [e.g., *Stott et al.*, 2000], depth of calcification [e.g., *Holsten et al.*, 2004], and ancient ocean circulation [e.g., *Wright and Miller*, 1993]. If the factors affecting $\delta^{13}C_{DIC}$ are carefully considered, $\delta^{13}C_{cc}$ records can provide the basis for determining the long-term history of $\delta^{13}C_{CO2}$. *Passey et al.* [2002] evaluated $\delta^{13}C_{CO2}$ for the past 20 million years from existing planktonic $\delta^{13}C$ records by applying a constant isotopic offset determined from seven planktonic foraminiferal species and near-modern atmosphere $\delta^{13}C_{CO2}$. A similar approach was used to re-evaluate Miocene $\delta^{13}C_{CO2}$ from benthic foraminiferal $\delta^{13}C$ records using a constant isotopic offset between benthic foraminifera and atmospheric CO_2 determined by comparing Pleistocene benthic foraminifera and pre-Industrial $\delta^{13}C_{CO2}$ [*Passey et al.*, 2009]. In general, these studies do not take into account the temporal sampling resolution of foraminiferal $\delta^{13}C$ variability, associations with photosymbiotes [*Spero*, 1992; *Spero and Lea*, 1993], downwelling rates and the strength of the biological pump [*Kroopnick*, 1985] — factors that increase the uncertainty in $\delta^{13}C_{CO2}$ reconstructions.

[6] Here, we present a meta-analysis of existing planktonic and benthic $\delta^{13}C_{cc}$ records and develop two proxy records of Cenozoic $\delta^{13}C_{CO2}$ values. We test the veracity of our approach by direct comparison with ice core $\delta^{13}C_{CO2}$ measurements spanning the last 50,000 years, and present a sensitivity analysis for uncertainties associated with diagenesis and temperature. The resulting $\delta^{13}C_{CO2}$ reconstructions of the past 65 million years are compared against each other and to other methodologies to reconstruct $\delta^{13}C_{CO2}$ values.

2. Summary of Methods

2.1. Benthic and Planktonic Foraminifera $\delta^{13}C$ and $\delta^{18}O$ Records

[7] We used 2,128 planktonic and 2,576 benthic foraminifera stable carbon ($\delta^{13}C_{cc}$) and oxygen ($\delta^{18}O_{cc}$) isotope measurements from 35 Deep Sea Drilling Project (DSDP), Ocean Drilling Program (ODP), and continental sites (Figure 1). Planktonic data was compiled from published articles (Table 1), whereas the benthic records are a subset of those compiled by *Zachos et al.* [2001]. The compiled records span the past 65 Myr and provide sample densities that resolve major paleoclimatic and paleoceanographic variation seen in the larger data sets of *Miller and Katz* [1987] and *Zachos et al.* [2001] (Figure 2). The restricted use of data reflects specific choices regarding foraminifera species and locations as discussed below.

[8] We limit our analysis to benthic genera *Cibicidoides* and *Nuttallides* [*Zachos et al.*, 2008, 2001] from the North Atlantic and Southern Oceans. Subtle differences between

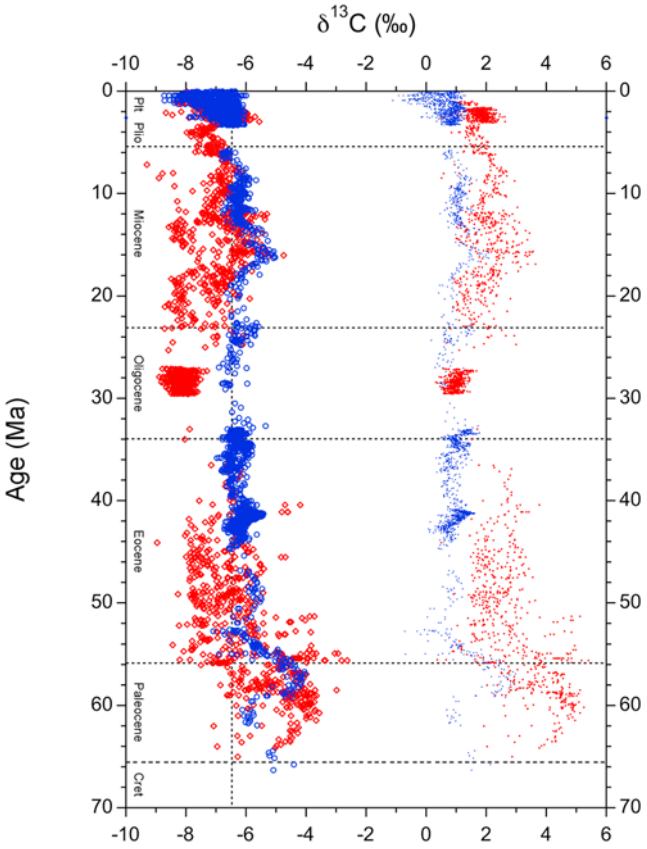

Figure 2. Raw foraminifera $\delta^{13}C_{cc}$ (dots) and reconstructed $\delta^{13}C_{CO2}$ (open symbols) over the past 65 Myr. Benthic foraminifera $\delta^{13}C_{cc}$ measurements (blue dots) and benthic-based $\delta^{13}C_{CO2}$ (blue circles) are shown with planktonic $\delta^{13}C_{cc}$ measurements (red dots) and planktonic-based $\delta^{13}C_{CO2}$ (red diamonds). Benthic foraminifera $\delta^{13}C_{cc}$ values reflect offsets used by *Zachos et al.* [2001]. Dashed line marks the pre-industrial $\delta^{13}C_{CO2}$ average of −6.5‰ [*Marino et al.*, 1992].

seawater and individual species $\delta^{13}C$ values increase the range of uncertainty of $\delta^{13}C_{CO2}$ produced from $\delta^{13}C$ records derived from multiple foraminiferal species. However, on multimillion year time scales, genera-specific adjustments are appropriate considering the limited geologic occurrence of individual species [*Hilting et al.*, 2008]. We adjusted *Nuttallides* $\delta^{13}C$ values in order to directly compare them to *Cibicidoides* values following the assumptions of *Katz et al.* [2003], where

$$\delta^{13}C_{Nutt-Cib} = \delta^{13}C_{Nutt} + 0.34. \quad (1)$$

To account for disequilibrium related to vital effects, *Cibicidoides* and *Nuttallides* $\delta^{18}O$ values were adjusted by +0.6‰ and +0.4‰, respectively [*Shackleton et al.*, 1984; *Zachos et al.*, 2001].

[9] Both *Cibicidoides* and *Nuttallides* are thought to be epifaunal genera [*Katz et al.*, 2003; *Thomas and Shackleton*, 1996]. However, recent work from *Sexton et al.* [2006a] suggests that both could have been shallow infaunal organisms. This slight infaunal behavior potentially protects these organisms from dissolution and better represents the isotopic character of bottom waters [*Katz et al.*, 2003; *Sexton et al.*, 2006a]. Overall, the available data indicate that *Cibicidoides* and *Nuttallides* genera provide a reliable proxy for the isotopic chemistry of ancient bottom waters.

[10] In our analysis, planktonic records are limited to surface-dwelling genera *Globigerinoides*, *Acarinina*, and *Morozovella*. Ancient *Globigerinoides*, *Acarinina*, and *Morozovella* are characterized by $\delta^{13}C_{cc}$ and $\delta^{18}O_{cc}$ values that are consistent with a surface dwelling habit [*Boersma et al.*, 1979; *Sexton et al.*, 2006b]. Extant *Globigerinoides, Acarinina,* and *Morozovella* species are associated with photosymbiotes, with an inverse relationship between test size and $\delta^{13}C$ value [*D'Hondt and Zachos*, 1993; *D'Hondt et al.*, 1994; *Pearson et al.*, 1993]. For this work, we do not attempt to correct for size effects in our planktonic foraminifera compilation, given that the isotopic effects are small (~0.2‰) and consistent size fraction sampling in older records is often lacking.

[11] We reviewed all existing age-depth relationship, updated age-depth relationships as needed, and placed all sites on an internally consistent age model using available magnetostratigraphic and biostratigraphic datums. All core age models are relative to the standard geomagnetic polarity time scale [*Cande and Kent*, 1995] and biostratigraphic datums for the Cenozoic [*Berggren et al.*, 1995].

2.2. Controls on DIC and Foraminiferal $\delta^{13}C$ Values

[12] Foraminiferal carbonate ($\delta^{13}C_{cc}$) is in approximate isotopic equilibrium with dissolved inorganic carbon ($\delta^{13}C_{DIC}$), roughly composed of 91% bicarbonate (HCO_3^-), 8% carbonate (CO_3^{2-}) and 1% carbonic acid (H_2CO_3) [*Zeebe and Wolf-Gladrow*, 2001]. Changes in the proportion of the dissolved carbonate species will influence foraminiferal $\delta^{13}C_{cc}$ values, and such changes are expected over time due to changes in the saturation state of calcium carbonate. If ocean pH changed during the Cenozoic from 7.6 to 8.2 in concert with changes in the ocean Mg/Ca ratio and the saturation state of $CaCO_3$ [*Tyrrell and Zeebe*, 2004], we estimate an isotopic effect of <−0.7‰ for $\delta^{13}C_{CO2}$ over tens of millions of years. Therefore, for simplicity, we assume that the proportion of each carbonate species is fixed over the Cenozoic.

[13] The balance between photosynthesis and air-sea mixing [*Gruber et al.*, 1999; *Lynch-Stieglitz et al.*, 1995] governs surface water $\delta^{13}C_{DIC}$ values. Photosynthesis and export productivity preferentially remove ^{12}C and lead to ^{13}C-enriched surface water DIC. In addition, cold surface water interactions with atmospheric CO_2 in high-latitude regions decrease the $^{13}C/^{12}C$ ratio of DIC [*Broecker and Maier-Reimer*, 1992]. These processes produce relatively stable spatial surface water $\delta^{13}C_{DIC}$ distributions that are offset from chemical equilibrium [*Gruber et al.*, 1999; *Lynch-Stieglitz et al.*, 1995]. For example, North Atlantic and Southern Ocean surface water $\delta^{13}C_{DIC}$ values are 1.0 ± 0.2‰ (1σ) more negative than those predicted by equilibrium calculations (Table 2).

[14] Export productivity and remineralization of organic carbon leads to water column $\delta^{13}C_{DIC}$ gradients [*Kroopnick*, 1985; *Lynch-Stieglitz et al.*, 1995]. North Atlantic and

Table 1. Cruise, Site, and Location Information for Published Foraminiferal Isotope Data Sets Used

DSDP/ODP Leg	DSDP/ODP Site	Latitude	Longitude	Basin	Location	Planktonic[a]	Benthic[a]	Sources[b]
6	44	19.31	−169.02	Central Pacific	Horizon Ridge	X		1
6	47	32.45	157.71	North Pacific	Shatsky Plateau	X		1
6	55	9.30	142.54	Central Pacific	Caroline Ridge	X		1
22	213	–10.21	93.90	Indian	Ninetyeast Ridge	X		2
22	215	–8.12	86.79	Indian	Ninetyeast Ridge	X		2
72	516	–30.28	–35.29	South Atlantic	Rio Grande Rise	X		1
73	524	–29.48	3.51	Central Atlantic	Walvis Ridge	X		3
74	525	–29.07	2.99	Central Atlantic	Walvis Ridge	X		4
74	526	–30.12	3.14	South Atlantic	Walvis Ridge	X		4
74	527	–28.04	1.76	Central Atlantic	Walvis Ridge	X		4
74	528	–28.52	2.32	Central Atlantic	Walvis Ridge	X		4
74	529	–28.93	2.77	Central Atlantic	Walvis Ridge	X		4
81	553	56.09	–23.34	North Atlantic	Rockall Plateau		X	5
82	558	37.77	–37.35	North Atlantic	Mid-Atlantic Ridge		X	6
82	563	33.64	–43.77	North Atlantic	Mid-Atlantic Ridge		X	7
85	572	1.43	–113.84	Central Pacific	Clipperton Fracture Zone	X		8
85	575	5.85	–135.04	Central Pacific	Clipperton Fracture Zone	X		9
90	590	–31.17	163.36	South Pacific	Lord Howe Rise	X		10
94	607	41.00	–32.96	North Atlantic	Mid-Atlantic Ridge		X	10
94	608	42.84	–23.09	North Atlantic	Mid-Atlantic Ridge	X	X	1, 7
113	689	–64.52	3.10	Southern	Maud Rise	X	X	11, 12, 13, 14
113	690	–65.17	1.22	Southern	Maud Rise	X	X	11, 12, 15
114	702	–49.87	–40.85	South Atlantic	Isla Orcadas Rise	X		2
117	730	17.73	57.69	Indian	Oman Margin	X		1
119	738	–62.72	82.78	Southern	Kerguelen Plateau	X	X	16
119	744	–61.23	80.59	Southern	Kerguelen Plateau		X	17
120	748	–58.44	78.98	Southern	Kerguelen Plateau		X	14, 18
121	757	–17.02	88.18	Indian	Ninetyeast Ridge	X		2
121	758	5.38	90.35	Indian	Ninetyeast Ridge	X		2
143	865	–18.43	–17.55	Central Atlantic	Allison Guyot	X		19
198	1209	32.65	158.50	North Pacific	Shatsky Rise	X		20
199	1218	8.89	–135.37	Central Pacific	Clipperton Fracture Zone	X		21
TDP[c]	NA[d]	–8.86	39.46	Indian		X		22

[a]Crosses mark if data are planktonic and/or benthic.
[b]Data sources for each data set are provided in Text S1.
[c]Continental Tanzania Drilling Project.
[d]NA, not applicable.

Southern Ocean deep-water $\delta^{13}C_{DIC}$ values proximal to modern downwelling zones are 1.2 ± 0.4‰ (1σ) more negative than surface water $\delta^{13}C_{DIC}$ (Table 2), and then become increasingly more negative with advection and age. Consequently, knowledge of past ocean circulation is required in order to restrict our evaluation of $\delta^{13}C_{CO2}$ to downwelling ocean sites with "young" ^{13}C-enriched deep waters. Early Cenozoic deep waters were primarily sourced from the Southern Ocean [*Via and Thomas*, 2006; *Wright and Miller*, 1993], with the gradual increase of northern-sourced deep waters from 33 Ma to present [*Davies et al.*, 2001; *Via and Thomas*, 2006]. Accordingly, we use Southern Ocean benthic foraminiferal $\delta^{13}C$ values between 65 and 33 Ma, and Northern Atlantic Ocean records between 33 Ma-present.

[15] Finally, the average infaunal benthic foraminifera $\delta^{13}C_{cc}$ values are 0.6 ± 0.3‰ (1σ) more negative than bottom water $\delta^{13}C_{DIC}$ values (Table 3). This mean value and its associated uncertainty are utilized in our long-term $\delta^{13}C_{CO2}$ reconstruction.

2.3. Reconstruction of $\delta^{13}C_{CO2}$ From Benthic Foraminifera $\delta^{13}C$

[16] The carbon isotopic composition of carbon dioxide in equilibrium with dissolved inorganic carbon is expressed as

$$\delta^{13}C_{CO_2(g)} = \left| \frac{\delta^{13}C_{DIC} + 10^3}{\left(\varepsilon_{DIC-CO_2(g)}/10^3\right) + 1} \right| - 10^3, \qquad (2)$$

Table 2. Coupled Surface and Bottom Water $\delta^{13}C_{DIC}$ Measurements, Air-Sea Surface Disequilibrium and Biologic Pump Offsets

	Measured Surface $\delta^{13}C_{DIC}$	Expected Surface $\delta^{13}C_{DIC}$	Measured Bottom $\delta^{13}C_{DIC}$	Air-Sea Surface Disequilibrium	Biologic Pump	Sources[a]
Mean (*n*)	2.0 (25)	3.0 (23)	0.8 (18)	1.0	1.2	23, 24
Standard Deviation	0.2	0.2	0.4	0.2	0.4	

[a]Sources presented in Text S1.

Table 3. Coupled Extant *Cibicidoides* Species $\delta^{13}C_{CC}$ and Bottom Water $\delta^{13}C_{DIC}$ Measurements

	Measured *Cibicidoides* spp. $\delta^{13}C_{CC}$	Measured Bottom $\delta^{13}C_{DIC}$	$\Delta\delta^{13}C$ (Remineralization/Oxidation)	Sources[a]
Mean (n)	0.3 (23)	0.9 (23)	0.6	25, 26, 27, 28, 29
Standard Deviation	0.2	0.1	0.3	

[a]Sources presented in Text S1.

where $\varepsilon_{DIC\text{-}CO2(g)}$ represents the empirical temperature-dependent fractionation factor between dissolved inorganic carbon and $CO_{2(g)}$ [*Zhang et al.*, 1995]:

$$\varepsilon_{DIC-CO_2(g)} = \left(0.91 \times \varepsilon_{HCO_3^- - CO_2(g)}\right) + \left(0.08 \times \varepsilon_{CO_3^{2-} - CO_2(g)}\right), \quad (3)$$

where

$$\varepsilon_{HCO_3^- - CO_2(g)} = -0.1141 \times T(^\circ C) + 10.78, \quad (4)$$

$$\varepsilon_{CO_3^{2-} - CO_2(g)} = 0.0049 \times T(^\circ C) - 1.31. \quad (5)$$

Carbon isotope compositions and ε values are expressed in per mil notation relative to the Pee Dee Belemnite (PDB) standard.

[17] Temperature is estimated from the oxygen isotopic composition of foraminiferal calcite following *Erez and Luz* [1983]:

$$T(^\circ C) = 17.0 - 4.52\left(\delta^{18}O_{cc} - \delta^{18}O_w\right) + 0.03\left(\delta^{18}O_{cc} - \delta^{18}O_w\right)^2, \quad (6)$$

where T is the calcification temperature, $\delta^{18}O_w$ is the oxygen isotopic composition of seawater, and $\delta^{18}O_{cc}$ the isotopic composition of the benthic foraminifera. High-latitude surface and deep-water temperatures are similar in downwelling zones [*Millero*, 2006], thus we assume calculated calcification temperatures from benthic species are similar to surface temperatures. Reconstructions of continental ice volumes [*Miller et al.*, 2005] were applied to estimate $\delta^{18}O_w$ through time. Our nominal solution uses $\delta^{18}O_w$ values of 0.0‰, −0.5‰, and −1.2‰ from the Present-5 Ma, 5–33 Ma, and 33–65 Ma, respectively. To evaluate the uncertainty in reconstructed deep-water temperature associated with (1) our model for $\delta^{18}O_w$ changes, and (2) potential diagenetic alteration of $\delta^{18}O_{cc}$, we present a series of sensitivity analyses in section 4.2.

[18] It should be noted that calculated $\delta^{13}C_{CO2}$ values are expected to be relatively insensitive to uncertainties related to estimated water temperatures. A ± 1‰ $\delta^{18}O_{cc}$ uncertainty reflects ~±4°C (from equation 6), corresponding to < ± 0.5‰ variation in $\delta^{13}C_{CO2}$. Considering that the entire Cenozoic range of $\delta^{18}O$ change is less than 6‰, our assumption of a three-step change in $\delta^{18}O_w$ makes a negligible difference in the calculation of $\delta^{13}C_{CO2}$. To account for surface water $\delta^{13}C_{DIC}$ distributions, export productivity, and the bacterial oxidation of organic carbon [*Corliss*, 1985], $\delta^{13}C$ values were increased by 1.0‰, 1.2‰, (Table 2), and 0.6‰, respectively. The above considerations yield the following expression for our $\delta^{13}C_{CO2}$ reconstruction from published benthic foraminifera [*Zachos et al.*, 2001]:

$$\delta^{13}C_{CO_2(g)} = \left\lfloor \frac{(\delta^{13}C_{CC} + \varepsilon_{DIC-CC} + A) + 10^3}{(\varepsilon_{DIC-CO_2(g)}/10^3) + 1} \right\rfloor - 10^3, \quad (7)$$

where A represents the sum total of disequilibrium effects from Tables 2 and 3 (surface water DIC disequilibrium, biological pump, and subsurface bacterial oxidation of organic material) related to biogenic carbonate production, equivalent to 2.8‰ for North Atlantic Ocean and Southern Ocean benthic foraminifera. The carbon isotope fractionation between calcium carbonate (calcite) and dissolved inorganic carbon is independent of temperature [*Romanek et al.*, 1992]:

$$\varepsilon_{DIC-CC} \approx -1‰. \quad (8)$$

We recognize that the magnitude of isotopic offsets applied could have been somewhat different in the past due to changes in ocean circulation and water mass production rates, but the range of uncertainty on $\delta^{13}C_{CO2}$ attributable to these effects is relatively small (see further discussion in section 4.2).

2.4. Reconstruction of $\delta^{13}C_{CO2}$ From Planktonic Foraminifera $\delta^{13}C$

[19] $\delta^{13}C_{CO2}$ can also be estimated from planktonic foraminifera $\delta^{13}C$ and $\delta^{18}O$. For this work, no adjustments for export productivity or bacterial oxidation of organic carbon were used for the surface-dwelling species. Given the highly localized nature of the ecosystems and microhabitats of planktonic foraminifera, it is difficult to constrain such factors in our global data set. The following relationship was used to estimate $\delta^{13}C_{CO2}$:

$$\delta^{13}C_{CO_2(g)} = \left\lfloor \frac{(\delta^{13}C_{CC} + \varepsilon_{DIC-CC}) + 10^3}{(\varepsilon_{DIC-CO_2(g)}/10^3) + 1} \right\rfloor - 10^3. \quad (9)$$

3. Results

3.1. Benthic Foraminifera-Based $\delta^{13}C_{CO2}$ Reconstruction

[20] Both planktic and benthic $\delta^{13}C_{cc}$ varied significantly over the Cenozoic, and it is likely $\delta^{13}C_{CO2}$ did so also (Figures 2 and 4 and auxiliary material).[1] Measured $\delta^{13}C_{CO2}$ values from ice cores over 50,000 years average −6.7‰ (range: −6.3 and −7.7‰) [*Elsig et al.*, 2009; *Friedli et al.*,

[1]Auxiliary material data sets are available at ftp://ftp.agu.org/apend/pa/2009pa001851.

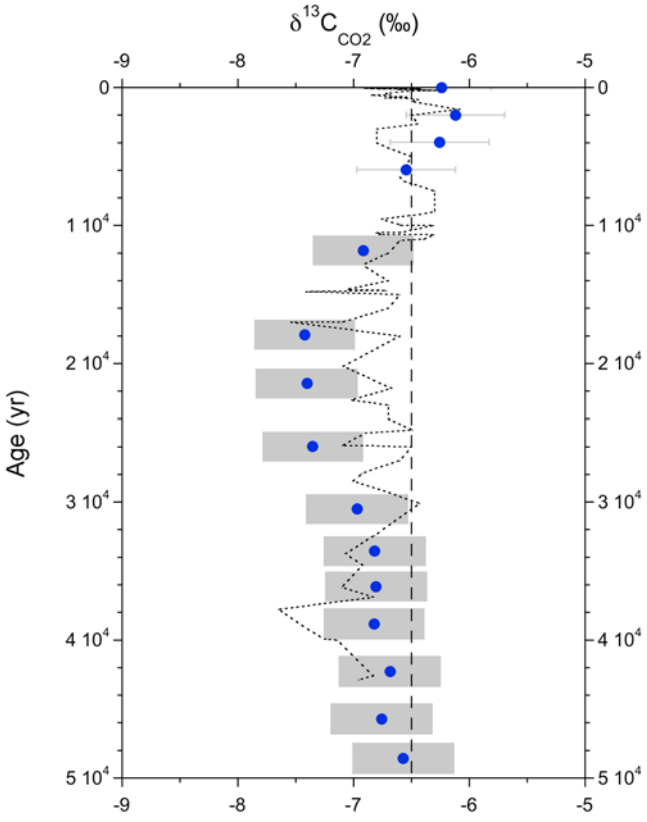

Figure 3. Given is $\delta^{13}C_{CO2}$ over the last 50 kyr. Direct measurements of $\delta^{13}C_{CO2}$ from CO_2 trapped in ice-core bubbles (dotted line) and benthic-based (blue) $\delta^{13}C_{CO2}$ estimates are shown with 95% confidence envelopes. Gray boxes surrounding the benthic-based $\delta^{13}C_{CO2}$ reconstructions greater than 10 kyr in age indicate a nominal temporal uncertainty of +/−1 kyr. The pre-industrial $\delta^{13}C_{CO2}$ average of −6.5‰ is shown with a dashed line [*Marino et al.*, 1992].

1986; *Leuenberger et al.*, 1992; *Smith et al.*, 1999], in accord with our benthic-based $\delta^{13}C_{CO2}$ results that average −6.8‰ (range: −6.1 and −7.4‰) (Figure 3). Furthermore, the benthic foraminifera-based $\delta^{13}C_{CO2}$ estimates accurately reconstruct measured $\delta^{13}C_{CO2}$ values for approximately 95% of the record (Figure 3). This is in good agreement with our statistical procedure, as we should expect that ~5% of the time the true $\delta^{13}C_{CO2}$ is not captured by the 95% confidence interval. Some of this disagreement may also be attributable to the fact that North Atlantic benthic foraminifera form their carbonate shells in bottom waters that were in contact with the atmosphere 50–400 years previously [*Broecker and Peng*, 1982; *Broecker et al.*, 1985]. Regardless, the observed accuracy across this time of profound climatic and oceanographic changes provides confidence that the assumptions we apply in our model are robust and applicable to more ancient geologic time intervals.

[21] Moving average $\delta^{13}C_{CO2}$ values for the entire Cenozoic are shown with 90% confidence intervals that incorporate the uncertainty associated with non-equilibrium effects and mean $\delta^{13}C_{cc}$ estimates (Figure 4 and Appendix A). Due to the widely variable sampling resolution of the benthic $\delta^{13}C_{cc}$ data, we dynamically adjust the number of points in the moving window in order to maintain a fixed temporal duration of 3 Myr. This approach contrasts with the typical *n*-point moving average, and is advantageous in this study because it more faithfully represents the true uncertainty associated with long-term changes in the average $\delta^{13}C_{cc}$; where data resolution is good, the 3 Myr uncertainty estimates are smaller because the mean value is well constrained. This approach provides a more geologically useful proxy for terrestrial paleoclimate and paleoecology applications (auxiliary material).

[22] The benthic-based $\delta^{13}C_{CO2}$ record averages −6.1 ± 0.6‰ (1σ) for the entire Cenozoic, similar to the commonly used pre-Industrial value of −6.5‰ (Figure 4). However, $\delta^{13}C_{CO2}$ also displays significant variations throughout the record, at times departing from the pre-Industrial value by more than 2‰. The most notable ^{13}C-enrichment (reaching −4‰) occurs between 61.5 to 52.8 Ma. Between 52.8 and 49.6 Ma, $\delta^{13}C_{CO2}$ was more positive by ~1‰ and returned

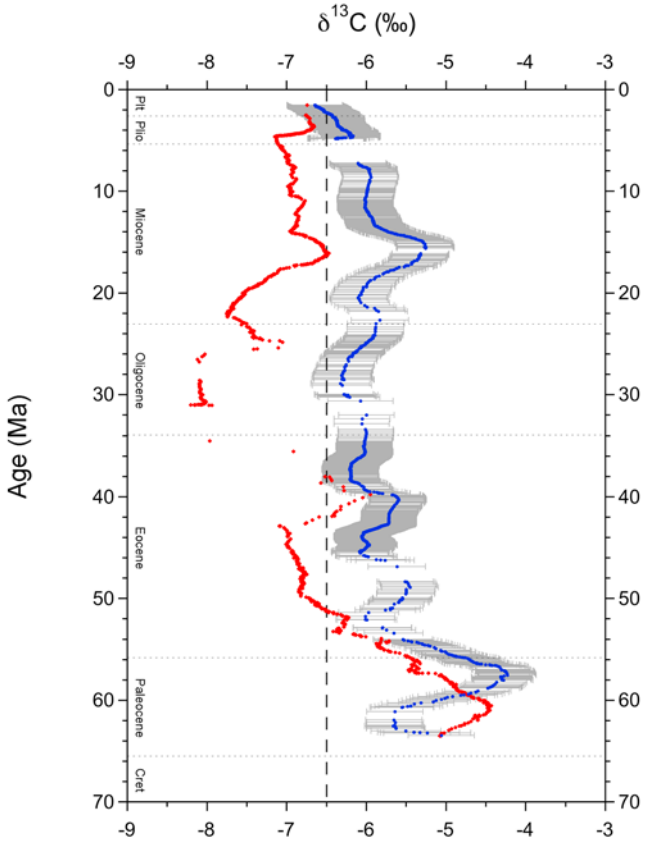

Figure 4. Cenozoic reconstructions of $\delta^{13}C_{CO2}$ from planktonic and benthic foraminiferal records. A 3 Myr-moving average benthic-based $\delta^{13}C_{CO2}$ reconstruction is shown in blue with 90% confidence intervals, and a 3 Myr-moving average planktonic-based $\delta^{13}C_{CO2}$ reconstruction is shown in red. No confidence intervals are assigned to the planktonic record because non-equilibrium factors affecting individual planktonic species cannot be rigorously quantified. The pre-industrial $\delta^{13}C_{CO2}$ average of −6.5‰ is shown with a dashed line [*Marino et al.*, 1992].

to the Cenozoic average value (−6.1‰) for the following ~32 Myr. The second largest enrichment, up to −5.3‰, occurs during peak warming of the Middle Miocene Climatic Optimum (17.3 to 14.5 Ma). $\delta^{13}C_{CO2}$ returned to −6.0 ± 0.5‰ between 12.9 to 7.9 Ma. From 7.9 to 5.3 Ma $\delta^{13}C_{CO2}$ values were ~0.5‰ more negative, and from 7.9 to 1.5 Ma $\delta^{13}C_{CO2}$ is characterized by a general decrease, achieving its lightest values of −6.6‰ in the most recent portion of the reconstruction. The Middle Miocene episode of ^{13}C-enrichment is particularly important for studies of ancient terrestrial-plant ecosystems, because it overlaps with the presumed time of C_4 grassland development (see section 4.3).

3.2. Planktonic Foraminifera-Based $\delta^{13}C_{CO2}$ Proxy Record

[23] Planktonic $\delta^{13}C_{cc}$ are more variable than the benthic $\delta^{13}C_{cc}$ record (Figure 2) and the 3 Ma moving average planktonic-based $\delta^{13}C_{CO2}$ time series is shown in Figure 4 (data provided within the auxiliary material). Confidence interval estimates are not provided because non-equilibrium factors affecting individual planktonic species cannot be rigorously quantified in a global compilation of this type. Planktonic $\delta^{13}C_{cc}$ captures similar trends as the benthic $\delta^{13}C_{cc}$ record with an average +1‰ offset. Planktonic-based $\delta^{13}C_{CO2}$ reconstructions average −6.9 ± 1.2‰ (1σ), ~0.4‰ more negative than the pre-Industrial value of −6.5‰ and 0.8‰ more negative than the benthic foraminifera-based $\delta^{13}C_{CO2}$ record (Figure 4). From 26.4 to 30.0 Ma a notably large offset (1–2‰) between planktonic- and benthic-based $\delta^{13}C_{CO2}$ reconstructions is observed (Figures 2 and 4). The planktonic-based $\delta^{13}C_{CO2}$ estimates during this interval are from a single species, *Globoquadrina venezuelana* at an equatorial Pacific locality (ODP 1218). While few studies of depth habitat have been performed for Oligocene species, limited data suggests *G. venezuelana* may live in the upper thermocline resulting in slightly more positive $\delta^{18}O_{cc}$ and more negative $\delta^{13}C_{cc}$ values than true surface-dwelling species [*Wade and Pälike*, 2004]. Nonetheless we include this data as it covers a large gap in the planktonic record.

4. Discussion

4.1. Comparison Between Benthic and Planktonic Foraminifera-Based $\delta^{13}C_{CO2}$

[24] Shallow-dwelling planktonic species are closely associated with the atmospheric CO_2 reservoir, but are subject to a variety of biologic, diagenetic, and temperature effects that vary in time and space and are difficult to constrain. Further, the planktonic $\delta^{13}C$ records in our complication have more limited temporal resolution and more isotopic variability (Figure 2) that add uncertainty to $\delta^{13}C_{CO2}$ estimates. For example, calculations of $\delta^{13}C_{CO2}$ performed for the Paleocene-Eocene Thermal Maximum use planktonic isotope records from ODP Sites 690 and 1209 [*Smith et al.*, 2007], and result in differences of 1.5–2.5‰ in the $\delta^{13}C_{CO2}$ value. Additional variability from Site 1209 is evident when $\delta^{13}C_{CO2}$ is estimated from both $\delta^{18}O_{cc}$ and Mg/Ca temperature estimates, yielding a difference of 1.0‰ in reconstructed $\delta^{13}C_{CO2}$ values. Further, temperature differences between planktonic foraminifera $\delta^{18}O_{cc}$ and the molecular temperature proxies $U^{K'}_{37}$ and TEX_{86} suggest surface water temperature differences of 3–5°C for the latest Eocene [*Liu et al.*, 2009], resulting in 0.4–0.6‰ variations in $\delta^{13}C_{CO2}$ depending on which temperature estimate is applied.

[25] The influence of photosymbionts, depth of production, and seasonal variability also affect the isotopic composition of planktonic foraminifera. *Spero* [1992] demonstrated that planktonic foraminifera grown under high-irradiance are as much as 3.7‰ more ^{13}C-enriched than the same species grown under ambient light. Seasonal variability and depth of production are difficult to constrain and lead to isotopic scatter in planktonic $\delta^{13}C_{cc}$ and $\delta^{18}O_{cc}$ data (Figure 2). Furthermore, the shallowest-dwelling species are not always available or easily identified in marine cores, and isotopic variability of shallow assemblages changes through time as new species emerge and others become extinct [*Hilting et al.*, 2008]. Since benthic species are not associated with photosymbionts and live exclusively in bottom waters they are free of these confounding effects.

[26] Finally, $\delta^{18}O_{cc}$ values of planktonic foraminifera can be altered due to recrystallization and incorporation of secondary calcite after burial. Diagenetic recrystallization and secondary cements increase the $\delta^{18}O_{cc}$ value of planktonic foraminifera, yielding lower apparent temperatures [*Schrag*, 1999]. While these diagenetic processes affect both planktonic and benthic foraminifera carbonate, they do not impact benthic isotope values to the same degree as benthic foraminifera are in near equilibrium with bottom water conditions.

[27] Given the large variability observed in the raw planktonic $\delta^{13}C_{cc}$ values (Figure 2) and the lack of a means to quantify the precise causes of this variability over large time intervals, we cannot assign reliable confidence intervals to these $\delta^{13}C_{CO2}$ estimates. We conclude that the benthic foraminiferal record provides a better estimate of ancient $\delta^{13}C_{CO2}$ over multimillion year timescales.

4.2. Sensitivity Analysis of Bottom Water Temperatures and Diagenesis

[28] To evaluate the impact of uncertainty in bottom water temperature on $\delta^{13}C_{CO2}$ estimates, we present two sensitivity analyses. The first of these sensitivity analyses utilizes a constant $\delta^{18}O_w$ value of 0.0‰. If the extreme assumption of a static $\delta^{18}O_w$ (0.0‰) is correct, $\delta^{13}C_{CO2}$ values are more ^{13}C-enriched by 0.2‰ between 5 and 33 Ma, and 0.5‰ between 33 and 65 Ma.

[29] In our nominal solution for $\delta^{13}C_{CO2}$ values, we assume that temperatures calculated from benthic foraminifera $\delta^{18}O_{cc}$ values are not subject to post-burial alteration, however, a general cooling trend is apparent across the Cenozoic. Thus, Paleogene-aged benthic foraminifera could have interacted with cooler Neogene bottom waters, promoting secondary alteration. Our second sensitivity analysis evaluates the influence of $\delta^{18}O_{cc}$ diagenesis by decreasing the bottom water temperatures by 2.5°C and increasing the measured $\delta^{18}O_{cc}$ values by 0.5‰ from 5 to 65 Ma. A 2.5°C increase in bottom water temperature decreases the nominal solution by 0.2‰ from 5 to 65 Ma (Figure 5). This sensi-

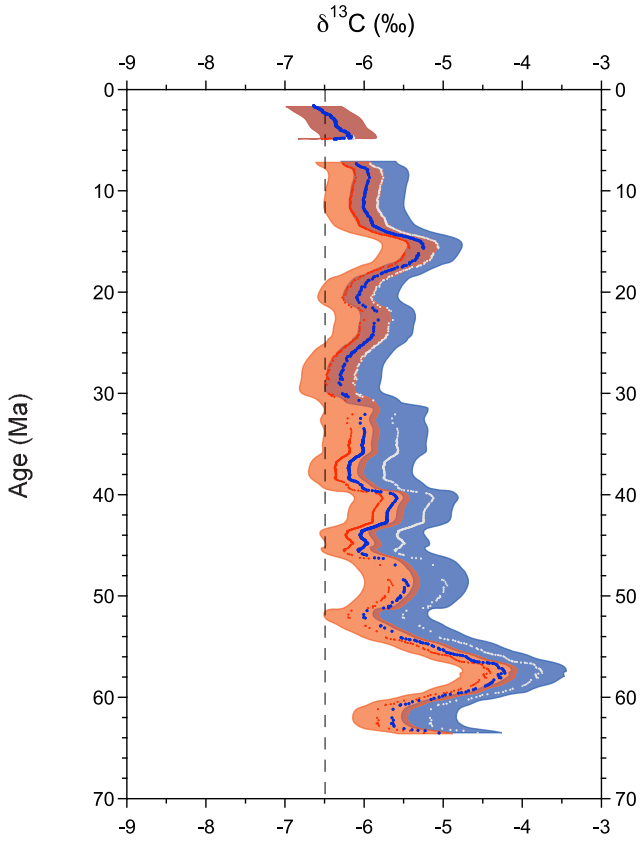

Figure 5. Sensitivity analysis of $\delta^{18}O_{cc}$ alteration and source water $\delta^{18}O_w$ variations on benthic-based $\delta^{13}C_{CO2}$ reconstructions. Nominal solution for $\delta^{13}C_{CO2}$ from Figure 4 shown with blue circles, while solutions for $\delta^{18}O_{cc}$ alteration and source water $\delta^{18}O_w$ variations are shown with red and grey circles respectively. The 90% confidence intervals for $\delta^{18}O_{cc}$ alteration and source water $\delta^{18}O_w$ solutions are shown with beige and blue envelopes. Brown regions indicate where both alteration and source water confidence intervals overlap.

tivity analysis does not include the last 5 Myr, which was the coldest of the Cenozoic Era, and thus bottom water temperatures would have had little effect on altering original $\delta^{18}O_{cc}$ values.

[30] The modeled variations in $\delta^{18}O_w$ and $\delta^{18}O_{cc}$ diagenesis result in opposing effects in the calculation of $\delta^{13}C_{CO2}$. As shown in Figure 5, the nominal solution is intermediate between the $\delta^{18}O_w$ and $\delta^{18}O_{cc}$ diagenesis sensitivity analyses results. The entire $\delta^{13}C_{CO2}$ range spanned by the 90% confidence intervals clearly excludes a pre-Industrial $\delta^{13}C_{CO2}$ value of −6.5‰ for much of the record. Furthermore, these results reveal that the general trends observed in the nominal solution are robust.

4.3. Impact of Atmospheric $\delta^{13}C_{CO2}$ Variations on Terrestrial Plant Reconstructions

[31] The rise of C_4 grassland in the Late Miocene/Pliocene, inferred from carbon isotope compositions of paleosols, soil carbonates, and fossil ungulate teeth [*Cerling et al.*, 1997; *Fox and Koch*, 2003, 2004; *Kingston et al.*, 1994; *Kleinert and Strecker*, 2001; *Morgan et al.*, 1994; *Passey et al.*, 2009, 2002], is arguably the most important terrestrial ecological event of the Neogene, with terrestrial C_4 expansion driven by a combination of regional climatic controls preconditioned by low pCO_2 levels [*Pagani et al.*, 1999; *Tipple and Pagani*, 2007]. Quantitative estimates of C_4 plant abundances are based on the carbon isotopic composition of terrestrial carbonates and/or organic matter, and require knowledge of the average C_3 and C_4 plant carbon-isotope compositions at any particular time. Our record indicates that $\delta^{13}C_{CO2}$ was −6.0‰ between 8 and 10 Ma and −5.2‰ during the Middle Miocene, roughly 0.5‰ and 1.3‰ more positive than the pre-Industrial value. Accordingly, average C_3 and C_4 plant carbon isotope compositions during these times were similarly ^{13}C-enriched.

[32] The presence of C_4 plants during the Early and Middle Miocene has been inferred from molecular clock data [*Christin et al.*, 2007; *Vicentini et al.*, 2008], with the Middle Miocene suggested to have been a major interval of C_4 diversification [*Vicentini et al.*, 2008]. Our benthic-based $\delta^{13}C_{CO2}$ reconstruction indicates that most published paleoecologic records covering these time periods are biased toward greater C_4 distribution because changes in $\delta^{13}C_{CO2}$ were not accounted for (Figure 4). For example, if a pre-Industrial $\delta^{13}C_{CO2}$ value is used to calculate C_4 contribution during the Middle Miocene, soil carbonate records from East Africa indicate between 10 and 36% C_4 biomass [*Kingston et al.*, 1994]. However, if the reconstructed $\delta^{13}C_{CO2}$ value of −5.2‰ is used for this interval, then C_4 contribution decreases to 0–18%. While these records continue to indicate C_4 plants were present during the Middle Miocene, new $\delta^{13}C_{CO2}$ reconstructions suggest C_4 grasses were less abundant than initially argued.

[33] Important changes in $\delta^{13}C_{CO2}$ appear to occur during the past ~10 Ma (Figures 2 and 4). The observed negative trend in $\delta^{13}C_{CO2}$ during this time has been previously interpreted as reflecting weathering of organic-rich rocks [*Shackleton*, 1987] — a supposition further supported by $^{187}Os/^{186}Os$ records [*Ravizza*, 1993]. However, other processes, such as a global expansion of terrestrial C_4 grasses and marine C_4-like pathways would have also impacted ocean $\delta^{13}C$ and $\delta^{13}C_{CO2}$ records [*Katz et al.*, 2005; *Kump and Arthur*, 1999]. Whatever the origin of the decrease in $\delta^{13}C_{cc}$ and $\delta^{13}C_{CO2}$, our data suggests that terrestrial ecologic reconstructions using carbon isotope ratios should include changes in $\delta^{13}C_{CO2}$ value in their discussions of plant community change.

5. Conclusions

[34] Two Cenozoic reconstructions of $\delta^{13}C_{CO2}$ are established from a meta-analysis of planktonic and benthic foraminiferal $\delta^{13}C$ and $\delta^{18}O$ records. We find that planktonic records have limited utility in the reconstruction of $\delta^{13}C_{CO2}$ across long geologic timescales due to lower temporal resolution and higher isotopic variability evident in modern species. High-resolution benthic foraminifera

$\delta^{13}C$ and $\delta^{18}O$ records constrain $\delta^{13}C_{CO2}$ values using a systematic treatment of environmental, diagenetic and species-specific effects, along with improved age models. Our results indicate that the Cenozoic was characterized by an average $\delta^{13}C_{CO2}$ value of −6.1‰ (~0.4‰ more positive than Pleistocene and pre-Industrial values). The resulting $\delta^{13}C_{CO2}$ record indicates pre-Industrial $\delta^{13}C_{CO2}$ and plant $\delta^{13}C$ values should not be assumed for most of the Cenozoic.

Appendix A: Atmospheric $\delta^{13}C_{CO2}$ Confidence Interval Estimation From Benthic Foraminifera $\delta^{13}C$

[35] Atmospheric $\delta^{13}C_{CO2}$ values and associated uncertainty are constrained by estimating mean values and 90% confidence intervals associated with four distinct variables: (1) benthic foraminiferal $\delta^{13}C$ ($\delta^{13}C_{cc}$), (2) the offset between $\delta^{13}C_{cc}$ and deep-water $\delta^{13}C$, attributable to the incorporation DIC from early diagenetic organic carbon remineralization ($\delta^{13}C_{cc\text{-}deep}$), (3) the surface-deep water offset associated with the biological pump ($\delta^{13}C_{surf\text{-}deep}$), and (4) the offset due to air-surface water disequilibrium ($\delta^{13}C_{air\text{-}surf}$).

[36] Three million year moving averages are calculated (Figure 4), following the application of species-specific corrections to benthic foraminiferal $\delta^{13}C$ measurements (Figure 2). In the algorithm utilized here, the number of points in the moving window is adjusted in order to maintain a fixed temporal duration. This approach is advantageous in this study, because the $\delta^{13}C_{cc}$ data set has widely variable sampling resolution. The 90% confidence interval for each 3 million year average is estimated as

$$\overline{\delta^{13}C_{CC}} + / - u_{cc}, \tag{A1}$$

$$u_{cc} = t^* \frac{S}{\sqrt{n}}, \tag{A2}$$

where $\overline{\delta^{13}C_{cc}}$ is the 3 million year average, u_{cc} is the uncertainty, s is the standard deviation, n is the number of data points in the window, and t^* is the upper 0.05 critical value associated with the $t(n\text{-}1)$ distribution.

[37] The 90% confidence intervals for $\overline{\delta^{13}C_{cc-deep}}$, $\overline{\delta^{13}C_{surf-deep}}$, and $\overline{\delta^{13}C_{air-surf}}$ are estimated in a similar fashion, using published $\delta^{13}C$ data (see Tables 2 and 3). The corresponding uncertainty estimates are designated $u_{cc\text{-}deep}$, $u_{surf\text{-}deep}$ and $u_{air\text{-}surf}$. To obtain a total uncertainty (u_{total}), the individual uncertainties are added in quadrature [*Taylor*, 1982]:

$$u_{total} = \sqrt{u_{cc}^2 + u_{cc-deep}^2 + u_{surf-deep}^2 + u_{air-surf}^2}. \tag{A3}$$

This total uncertainty is utilized to in equation 7 to estimate $\delta^{13}C_{CO2}$ uncertainty from the measured benthic foraminiferal $\delta^{13}C$ data. Benthic temperature estimates determined in equation 6 utilize $\delta^{18}O_{cc}$ from this same set of benthic foraminifera, and are also smoothed with the 3 Myr moving average procedure.

[38] **Acknowledgments.** We wish to thank M. Hren, K. Turekian, and D. Zinniker for helpful discussions. In addition, we would like to acknowledge P. Koch, J. Hayes, L. Kump, G. Dickens, B. Passey, and two anonymous reviewers for their thoughtful and constructive comments that greatly improved this work.

References

Berggren, W. A., et al. (1995), A revised Cenozoic geochronology and chronostratigraphy, in *Geochronology Time Scales and Global Stratigraphic Correlation*, edited by W. A. Berggren et al., pp. 129–212, Soc. for Sediment. Geol., Tulsa, Okla.

Berner, R. A. (1998), The carbon cycle and carbon dioxide over Phanerozoic time: The role of land plants, *Philos. Trans. R. Soc. London, Ser. B*, *353*, 75–82, doi:10.1098/rstb.1998.0192.

Berner, R. A. (2006), GEOCARBSULF: A combined model for Phanerozoic atmospheric O_2 and CO_2, *Geochim. Cosmochim. Acta*, *70*, 5653–5664, doi:10.1016/j.gca.2005.11.032.

Bibi, F. (2007), Dietary niche partitioning among fossil bovids in late Miocene C_3 habitats: Consilience of functional morphology and stable isotope analysis, *Palaeogeogr. Palaeoclimatol. Palaeoecol.*, *253*, 529–538, doi:10.1016/j.palaeo.2007.06.014.

Boersma, A., et al. (1979), Carbon and oxygen isotope records at DSDP Site 384 (North Atlantic) and some Paleocene paleotemperatures and carbon isotope variations in the Atlantic Ocean, *Initial Rep. Deep Sea Drill. Proj.*, *43*, 695–717.

Boisserie, J.-R., et al. (2005), Diets of modern and late Miocene hippopotamids: Evidence from carbon isotope composition and micro-wear of tooth enamel, *Palaeogeogr. Palaeoclimatol. Palaeoecol.*, *221*, 153–174, doi:10.1016/j.palaeo.2005.02.010.

Broecker, W. S., and E. Maier-Reimer (1992), The influence of air and sea exchange on the carbon isotope distribution in the sea, *Global Biogeochem. Cycles*, *6*, 315–320, doi:10.1029/92GB01672.

Broecker, W. S., and T.-H. Peng (1982), *Tracers in the Sea*, Lamont-Doherty Geol. Obs., Palisades, N. Y.

Broecker, W. S., T.-H. Peng, G. Ostlund, and M. Stuiver (1985), The distribution of bomb radiocarbon in the ocean, *J. Geophys. Res.*, *90*, 6953–6970, doi:10.1029/JC090iC04p06953.

Bump, J. K., et al. (2007), Stable isotopes, ecological integration and environmental change: Wolves record atmospheric carbon isotope trend better than tree rings, *Proc. R. Soc. B*, *274*, 2471–2480, doi:10.1098/rspb.2007.0700.

Cande, S. C., and D. V. Kent (1995), Revised calibration of the geomagnetic polarity timescale for the Late Cretaceous and Cenozoic, *J. Geophys. Res.*, *100*, 6093–6095, doi:10.1029/94JB03098.

Cerling, T. E., et al. (1997), Global vegetation change through the Miocene/Pliocene boundary, *Nature*, *389*, 153–158, doi:10.1038/38229.

Christin, P.-A., et al. (2007), C_4 photosynthesis evolved in grasses via parallel adaptive genetic changes, *Curr. Biol.*, *17*, 1241–1247, doi:10.1016/j.cub.2007.06.036.

Corliss, B. H. (1985), Microhabitats of benthic foraminifera within deep-sea sediments, *Nature*, *314*, 435–438, doi:10.1038/314435a0.

Davies, R., et al. (2001), Early Oligocene initiation of North Atlantic Deep Water formation, *Nature*, *410*, 917–920, doi:10.1038/35073551.

Deines, P. (1980), The isotopic composition of reduced organic carbon, in *Handbook of Environmental Isotope Geochemistry: I. The Terrestrial Environment*, edited by P. Fritz and J. C. Fontes, pp. 329–406, Elsevier, Amsterdam.

D'Hondt, S., and J. C. Zachos (1993), On stable isotopic variation and earliest Paleocene planktonic foraminifera, *Paleoceanography*, *8*, 527–547, doi:10.1029/93PA00952.

D'Hondt, S., et al. (1994), Stable isotopic signals and photosymbiosis in Late Paleocene planktic foraminifera, *Paleobiology*, *20*, 391–406.

Elsig, J., et al. (2009), Stable isotope constraints on Holocene carbon cycle changes from an Antarctic ice core, *Nature*, *461*, 507–510, doi:10.1038/nature08393.

Erez, J., and B. Luz (1983), Experimental paleotemperature equation for planktonic foraminifera, *Geochim. Cosmochim. Acta*, *47*, 1025–1031, doi:10.1016/0016-7037(83)90232-6.

Farquhar, G. D., et al. (1989), Carbon isotope discrimination and photosynthesis, *Annu. Rev. Plant Physiol. Plant Mol. Biol.*, *40*, 503–537, doi:10.1146/annurev.pp.40.060189.002443.

Feakins, S. J., et al. (2005), Biomarker records of late Neogene changes in northeast Africa vegetation, *Geology*, *33*, 977–980, doi:10.1130/G21814.1.

Feakins, S. J., et al. (2007), A comparison of biomarker records of northeast African vegetation from lacustrine and marine sediments (ca. 3.40 Ma), *Org. Geochem.*, *38*, 1607–1624, doi:10.1016/j.orggeochem.2007.06.008.

Follett, R. F., et al. (2009), No-till corn after bromegrass: Effect on soil carbon and soil aggregates, *Agron. J.*, *101*, 261–268, doi:10.2134/agronj2008.0107.

Fox, D. L., and P. L. Koch (2003), Tertiary history of C_4 biomass in the Great Plains, USA, *Geology*, *31*, 809–812, doi:10.1130/G19580.1.

Fox, D. L., and P. L. Koch (2004), Carbon and oxygen isotopic variability in Neogene paleosol carbonates: Constraints on the evolution of the C_4-grasslands of the Great Plains, USA, *Palaeogeogr. Palaeoclimatol. Palaeoecol.*, *207*, 305–329, doi:10.1016/S0031-0182(04)00045-8.

Friedli, H., et al. (1986), Ice core record of the $^{13}C/^{12}C$ ratio of atmospheric CO_2 in the past two centuries, *Nature*, *324*, 237–238, doi:10.1038/324237a0.

Gröcke, D. R. (2002), The isotopic composition of ancient CO_2 based on higher-plant organic matter, *Philos. Trans. R. Soc. London, Ser. A*, *360*, 633–658, doi:10.1098/rsta.2001.0965.

Gruber, N., C. D. Keeling, R. B. Bacastow, P. R. Guenther, T. J. Lueker, M. Wahlen, H. A. J. Meijer, W. G. Mook, and T. F. Stocker (1999), Spatiotemporal patterns of carbon-13 in the global surface oceans and the oceanic Suess effect, *Global Biogeochem. Cycles*, *13*, 307–335, doi:10.1029/1999GB900019.

Hilting, A. K., L. R. Kump, and T. J. Bralower (2008), Variations in the oceanic vertical carbon isotope gradient and their implications for the Paleocene-Eocene biological pump, *Paleoceanography*, *23*, PA3222, doi:10.1029/2007PA001458.

Holsten, J., et al. (2004), Reconstructing benthic carbon oxidation rates using $\delta^{13}C$ of benthic foraminifers, *Mar. Micropaleontol.*, *53*, 117–132, doi:10.1016/j.marmicro.2004.05.006.

Hopley, P. J., et al. (2007), Orbital forcing and the spread of C_4 grasses in the late Neogene: Stable isotope evidence from South African speleothems, *J. Hum. Evol.*, *53*, 620–634, doi:10.1016/j.jhevol.2007.03.007.

Jahren, A. H., et al. (2001), Terrestrial record of methane hydrate dissociation in the Early Cretaceous, *Geology*, *29*, 159–162, doi:10.1130/0091-7613(2001)029<0159:TROMHD>2.0.CO;2.

Katz, M. E., D. R. Katz, J. D. Wright, K. G. Miller, D. K. Pak, N. J. Shackleton, and E. Thomas (2003), Early Cenozoic benthic foraminiferal isotopes: Species reliability and interspecies correction factors, *Paleoceanography*, *18*(2), 1024, doi:10.1029/2002PA000798.

Katz, M. E., et al. (2005), Biological overprint of the geological carbon cycle, *Mar. Geol.*, *217*, 323–338, doi:10.1016/j.margeo.2004.08.005.

Kingston, J. D., et al. (1994), Isotopic evidence for Neogene hominid paleoenvironments in the Kenya Rift Valley, *Science*, *264*, 955–959, doi:10.1126/science.264.5161.955.

Kleinert, K., and M. R. Strecker (2001), Climate change in response to orographic barrier uplift: Paleosol and stable isotope evidence from the late Neogene Santa Maria basin, northwestern Argentina, *Geol. Soc. Am. Bull.*, *113*, 728–742, doi:10.1130/0016-7606(2001)113<0728:CCIRTO>2.0.CO;2.

Kroopnick, P. M. (1985), The distribution of ^{13}C of ΣCO_2 in the world oceans, *Deep Sea Res., Part A*, *32*, 57–84, doi:10.1016/0198-0149(85)90017-2.

Kump, L. R., and M. A. Arthur (1999), Interpreting carbon-isotope excursions: Carbonates and organic matter, *Chem. Geol.*, *161*, 181–198, doi:10.1016/S0009-2541(99)00086-8.

Lai, C.-T., W. Riley, C. Owensby, J. Ham, A. Schauer, and J. R. Ehleringer (2006), Seasonal and interannual variations of carbon and oxygen isotopes of respired CO_2 in a tallgrass prairie: Measurements and modeling results from 3 years with contrasting water availability, *J. Geophys. Res.*, *111*, D08S06, doi:10.1029/2005JD006436.

Leuenberger, M., et al. (1992), Carbon isotope composition of atmospheric CO_2 during the last ice age from an Antarctic core, *Nature*, *357*, 488–490, doi:10.1038/357488a0.

Levin, N. E., et al. (2004), Isotopic evidence for Plio-Pleistocene environmental change at Gona, Ethiopia, *Earth Planet. Sci. Lett.*, *219*, 93–110, doi:10.1016/S0012-821X(03)00707-6.

Liu, Z., et al. (2009), Global cooling during the Eocene-Oligocene climate transition, *Science*, *323*, 1187–1190, doi:10.1126/science.1166368.

Lynch-Stieglitz, J., T. F. Stocker, W. S. Broecker, and R. G. Fairbanks (1995), The influence of air-sea exchange on the isotopic composition of oceanic carbon: Observations and modeling, *Global Biogeochem. Cycles*, *9*, 653–665, doi:10.1029/95GB02574.

Marino, B. D., et al. (1992), Glacial-to-interglacial variations in the carbon isotopic composition of atmospheric CO_2, *Nature*, *357*, 461–466, doi:10.1038/357461a0.

Miller, K. G., and M. E. Katz (1987), Oligocene to Miocene benthic foraminiferal and abyssal circulation changes in the North Atlantic, *Micropaleontology*, *33*, 97–149, doi:10.2307/1485489.

Miller, K. G., et al. (2005), The Phanerozoic record of global sea-level change, *Science*, *310*, 1293–1298, doi:10.1126/science.1116412.

Millero, F. J. (2006), *Chemical Oceanography*, 3rd ed., 496 pp., Taylor and Francis, Boca Raton, Fla.

Morgan, M. E., et al. (1994), Carbon isotopic evidence for the emergence of C_4 plants in the Neogene from Pakistan and Kenya, *Nature*, *367*, 162–165, doi:10.1038/367162a0.

Pagani, M., M. A. Arthur, and K. H. Freeman (1999), Miocene evolution of atmospheric carbon dioxide, *Paleoceanography*, *14*, 273–292, doi:10.1029/1999PA900006.

Pagani, M., et al. (2005), Marked decline in atmospheric carbon dioxide concentrations during the Paleogene, *Science*, *309*, 600–603, doi:10.1126/science.1110063.

Passey, B. H., et al. (2002), Environmental change in the Great Plains: An isotopic record from fossil horses, *J. Geol.*, *110*, 123–140, doi:10.1086/338280.

Passey, B. H., et al. (2009), Strengthened East Asian summer monsoons during a period of high-latitude warmth? Isotopic evidence from Mio-Pliocene fossil mammals and soil carbonates from northern China, *Earth Planet. Sci. Lett.*, *277*, 443–452, doi:10.1016/j.epsl.2008.11.008.

Pearson, P. N., et al. (1993), Stable isotope paleoecology of Middle Eocene planktonic foraminifera and multi-species isotope stratigraphy, DSDP Site 523, South Atlantic, *J. Foraminiferal Res.*, *23*, 123–140, doi:10.2113/gsjfr.23.2.123.

Pypker, T. G., et al. (2008), Toward using $\delta^{13}C$ of ecosystem respiration to monitor canopy physiology in complex terrain, *Oecologia*, *158*, 399–410, doi:10.1007/s00442-008-1154-3.

Ravizza, G. (1993), Variations of the $^{187}Os/^{186}Os$ ratio of seawater over the past 28 million years as inferred from metalliferous carbonates, *Earth Planet. Sci. Lett.*, *118*, 335–348, doi:10.1016/0012-821X(93)90177-B.

Romanek, C. S., et al. (1992), Carbon isotopic fractionation in synthetic aragonite and calcite effects of temperature and precipitation rate, *Geochim. Cosmochim. Acta*, *56*, 419–430, doi:10.1016/0016-7037(92)90142-6.

Royer, D. L., et al. (2004), CO_2 as a primary driver of Phanerozoic climate change, *GSA Today*, *14*, 4–10.

Schrag, D. P. (1999), Effects of diagenesis on the isotopic record of late Paleogene tropical sea surface temperatures, *Chem. Geol.*, *161*, 215–224, doi:10.1016/S0009-2541(99)00088-1.

Ségalen, L., et al. (2006), Neogene climate change and emergence of C_4 grasses in the Namib, southwestern Africa, as reflected in ratite ^{13}C and ^{18}O, *Earth Planet. Sci. Lett.*, *244*, 725–734, doi:10.1016/j.epsl.2005.12.012.

Sexton, P. F., P. A. Wilson, and R. D. Norris (2006a), Testing the Cenozoic multisite composite $\delta^{18}O$ and $\delta^{13}C$ curves: New monospecific Eocene records from a single locality, Demerara Rise (Ocean Drilling Program Leg 207), *Paleoceanography*, *21*, PA2019, doi:10.1029/2005PA001253.

Sexton, P. F., et al. (2006b), Palaeoecology of late middle Eocene planktic foraminifera and evolutionary implications, *Mar. Micropaleontol.*, *60*, 1–16, doi:10.1016/j.marmicro.2006.02.006.

Shackleton, N. J. (1987), The carbon isotope record of the Cenozoic: History of organic carbon burial and of oxygen in the ocean and atmosphere, in *Marine Petroleum Source Rocks*, edited by J. Brooks and A. J. Fleet, *Geol. Soc. Spec. Publ.*, 26, 423–434.

Shackleton, N. J., et al. (1984), Oxygen and carbon isotope data from Leg 74 foraminifers, *Initial Rep. Deep Sea Drill. Proj.*, *74*, 599–612.

Smith, F. A., et al. (2007), Magnitude of the carbon isotope excursion at the Paleocene-Eocene thermal maximum: The role of plant community change, *Earth Planet. Sci. Lett.*, *262*, 50–65, doi:10.1016/j.epsl.2007.07.021.

Smith, H. J., et al. (1999), Dual modes of the carbon cycle since the Last Glacial Maximum, *Nature*, *400*, 248–250, doi:10.1038/22291.

Spero, H. J. (1992), Do planktic foraminifera accurately record shifts in the carbon isotopic composition of seawater ΣCO_2?, *Mar. Micropaleontol.*, *19*, 275–285, doi:10.1016/0377-8398(92)90033-G.

Spero, H. J., and D. W. Lea (1993), Instraspecific stable isotope variability in the planktic foraminiferal *Globigerinoides sacculifer*: Results from laboratory experiments, *Mar. Micropaleontol.*, *22*, 221–234, doi:10.1016/0377-8398(93)90045-Y.

Stott, L. D., et al. (2000), Increased dissolved oxygen in Pacific intermediate waters due to lower rates of carbon oxidation in sediments, *Nature*, *407*, 367–370, doi:10.1038/35030084.

Taylor, J. R. (1982), *An Introduction to Error Analysis*, 327 pp., Univ. Sci. Books, Mill Valley, Calif.

Thomas, E., and N. J. Shackleton (1996), The Paleocene-Eocene benthic foraminiferal extinction and stable isotope anomalies, in *Correlation of the Early Paleogene in Northwest Europe*, edited by R. W. O'B. Knox, R. M. Corfield, and R. E. Dunay, *Geol. Soc. Spec. Publ.*, 101, 401–441.

Tipple, B. J., and M. Pagani (2007), The early origins of terrestrial C_4 photosynthesis, *Annu. Rev. Earth Planet. Sci.*, *35*, 435–461, doi:10.1146/annurev.earth.35.031306.140150.

Tyrrell, T., and R. E. Zeebe (2004), History of carbonate ion concentration over the last 10 million years, *Geochim. Cosmochim. Acta*, *68*, 3521–3530, doi:10.1016/j.gca.2004.02.018.

van Bergen, P. F., and I. Poole (2002), Stable carbon isotopes of wood: A clue to palaeoclimate?, *Palaeogeogr. Palaeoclimatol. Palaeoecol.*, *182*, 31–45, doi:10.1016/S0031-0182(01)00451-5.

Via, R. K., and D. J. Thomas (2006), Evolution of Atlantic thermohaline circulation: Early Oligocene onset of deep-water production in the North Atlantic, *Geology*, *34*, 441–444, doi:10.1130/G22545.1.

Vicentini, A., J. C. Barber, S. S. Aliscioni, L. M. Giussani, and E. A. Kellogg (2008), The age of the grasses and clusters of origins of C_4 photosynthesis, *Global Change Biol.*, *14*, 2963–2977, doi:10.1111/j.1365-2486.2008.01688.x.

Wade, B. S., and H. Pälike (2004), Oligocene climate dynamics, *Paleoceanography*, *19*, PA4019, doi:10.1029/2004PA001042.

Wang, L., et al. (2010), Patterns and implications of plant-soil $\delta^{13}C$ and $\delta^{15}N$ values in African savanna ecosystems, *Quat. Res.*, *73*, 77–83, doi:10.1016/j.yqres.2008.11.004.

Wright, J. D., and K. G. Miller (1993), Southern Ocean influence on Late Eocene to Miocene deep-water circulation, in *The Antarctic Paleoenvironment: A Perspective on Global Change, Part 2*, *Antarct. Res. Ser.*, vol. 60, edited by J. P. Kennett and D. A. Warnke, pp. 1–25, AGU, Washington, D. C.

Zachos, J. C., et al. (2001), Trends, rhythms, and aberrations in global climate 65 Ma to present, *Science*, *292*, 686–693, doi:10.1126/science.1059412.

Zachos, J. C., et al. (2008), An early Cenozoic perspective on greenhouse warming and carbon-cycle dynamics, *Nature*, *451*, 279–283, doi:10.1038/nature06588.

Zazzo, A., et al. (2000), Herbivore paleodiet and paleoenvironmental changes in Chad during the Pliocene using stable isotope ratios of tooth enamel carbonate, *Paleobiology*, *26*, 294–309, doi:10.1666/0094-8373(2000)026<0294:HPAPCI>2.0.CO;2.

Zeebe, R. E., and D. A. Wolf-Gladrow (2001), *CO_2 in Seawater: Equilibrium, Kinetics, Isotopes*, 346 pp., Elsevier, Amsterdam.

Zhang, J., et al. (1995), Carbon-isotope fractionation during gas-water exchange and dissolution of CO_2, *Geochim. Cosmochim. Acta*, *59*, 107–114, doi:10.1016/0016-7037(95)91550-D.

S. R. Meyers, Department of Geoscience, University of Wisconsin-Madison, Madison, WI 53706, USA. (smeyers@geology.wisc.edu)

M. Pagani, Department of Geology and Geophysics, Yale University, New Haven, CT 06520, USA. (mark.pagani@yale.edu)

B. J. Tipple, Department of Biology, University of Utah, Salt Lake City, UT 84112, USA. (brett.tipple@utah.edu)